OPEN ACCESS

Short report

Using long-read sequencing to detect and subtype a case with Temple syndrome

Sarah Dada ,[1,2] Vahid Akbari ,[1,3] Duha Hejla,[4,5] Yaoqing Shen,[1] Katherine Dixon,[1,3] Sanaa Choufani,[6] Rosanna A Weksberg,[6,7] Cornelius F Boerkoel,[3,8] Laura Stewart,[4,5] Kamilla Schlade-Bartusiak,[9,10] Emma Strong,[9] Danya Fox,[4,5] Daniel Gamu,[3,11] William T Gibson ,[3,4,8,10] Steven J M Jones[1,2,3]

► Additional supplemental material is published online only. To view, please visit the journal online (https://doi.org/10.1136/jmg-2024-110262).

For numbered affiliations see end of article.

Correspondence to
Dr Steven J M Jones;
sjones@bcgsc.ca

SD and VA contributed equally.

Received 19 July 2024
Accepted 7 May 2025

To cite: Dada S, Akbari V, Hejla D, *et al*. *J Med Genet* Epub ahead of print: [please include Day Month Year]. doi:10.1136/jmg-2024-110262

ABSTRACT

Temple syndrome is an imprinting disorder resulting from abnormal genomic or epigenomic aberrations of chromosome 14 including maternal uniparental disomy (matUPD), paternal deletion of 14q32, or aberrant methylation of the imprinting control regions at 14q32. Understanding the underlying molecular mechanism is essential to understanding the recurrence risk and physical effects. Currently, diagnosis requires the detection of aberrant methylation and copy number loss via methylation-sensitive assays such as methylation-specific multiplex ligation-dependent probe amplification, and short tandem repeat analysis to detect matUPD and the presence of epimutation. Therefore, a one-step approach that can detect aberrant methylation and underlying genetic mechanisms would be of high clinical value. Here we use nanopore sequencing to delineate the molecular diagnosis of a case with Temple syndrome. We demonstrate the application of nanopore sequencing to detect aberrant methylation and underlying genetic mechanisms simultaneously in this case, thus providing a proof of concept for a one-step approach for molecular diagnosis of this disorder.

INTRODUCTION

Temple syndrome (TS) is a rare imprinting disorder characterised by early neonatal hypotonia, feeding problems, delayed motor milestones, growth retardation, small hands and feet, precocious puberty, and adult short stature.[1 2] Some patients develop truncal obesity or early onset type 2 diabetes. Cognitive development ranges from moderately delayed to normal.[1] Temple syndrome is caused by abnormal expression of imprinted genes at the 14q32 region. A primary cause of Temple syndrome is maternal uniparental disomy (matUPD), including maternal heterodisomy, maternal isodisomy and mixed matUPD. Additionally, aberrant methylation of imprinted differentially methylated regions (iDMRs) such as the *MEG3/DLK1* (IG-DMR) and *MEG3*:TSS-DMR imprinting control regions (ICRs) can cause Temple syndrome, as can deletion of the paternal region at 14q32.[1 3 4] Early diagnosis and treatment of Temple syndrome is important to optimise long-term outcomes and quality of life.[2 5] Moreover, it has been suggested that different molecular mechanisms leading to TS may confer reproducible differences in phenotype, such that endophenotypes may exist,[6] and as such that determination of the Temple syndrome molecular subtype would enhance ideal clinical management.

Clinical-grade molecular diagnosis of Temple syndrome may require more than one technique: methylation-specific multiplex ligation-dependent probe amplification (MS-MLPA), methylation-specific PCR for methylation status, and chromosomal microarray may be used to find UPD and/or deletions of the critical region among patients. Joint testing of the patient and their parents using polymorphic markers such as short tandem repeat (STR) markers may also be deemed necessary.

Currently, MS-MLPA is often recommended to assess both imprinting aberrations and deletions.[7] Additionally, microsatellite marker analysis, exome sequencing or short-read whole genome sequencing can also identify matUPD,[1 8 9] but parental samples are often required for definitive molecular resolution. Oxford Nanopore Technology (ONT) long-read sequencing allows the simultaneous detection of sequence variants and DNA methylation status. Additionally, the long reads usually encompass multiple heterozygous variants that enable read phasing and detection of allele-specific events.[10] Yamada *et al* and our group have demonstrated the use of long reads in the molecular diagnosis of imprinting disorders Prader-Willi syndrome and Angelman syndrome.[11 12] In this study, we applied nanopore sequencing to resolve the molecular cause of Temple syndrome in a patient who had previously been diagnosed using clinical diagnostic methods. We successfully confirmed the methylation status of the *MEG3/DLK1* (IG-DMR) and *MEG3*:TSS-DMR ICRs, the lack of structural variants in the *MEG3* region, and the presence of maternal isodisomy at the TS critical region without parental data. Additionally, we detected a proximal heterozygous region at chromosome 14 (Chr14) with biparental inheritance, concordant with prior genetic testing. Our results demonstrate that long-read sequencing can be used as a one-step approach to replace conventional tests for the diagnosis of Temple syndrome.

METHODS

Participant information and clinical testing

The participant was a female patient in middle childhood followed clinically at British Columbia

Table 1 Laboratory and dual-energy X-ray absorptiometry (DEXA) studies. Cortisol was drawn the morning of testing. Internal reference data calibrated against National Health and Nutrition Examination Survey (NHANES) data.[13] Fat-free mass includes both lean tissue mass and bone mineral content (BMC). The centiles of per cent body fat (rightmost column) are estimated based on data matched to chronological age. Android and gynoid fat, fat-free and total masses reflect sex-biased mass distribution calibrated against patients not known to have rare genetic and/or epigenetic disorders. Note that the pubertal hormone reference ranges are age-based and thus may flag as elevated given her advanced pubertal status

Laboratory studies								
Chronological age (approximate time points)	**Time point 3**		**Time point 4**		**Time point 8**		**Time point 9**	
Hormone (units)	**Value**	**Reference range**	**Value**	**Reference range**	**Value**	**Reference range**	**Value**	**Reference range**
Thyroid-stimulating hormone (TSH) (mU/L)	2.06	0.35–5.50	1.63	0.35–5.50				
Free thyroxine (fT4) (pmol/l)	n.d.		8.3	7.9–14.4				
Cortisol (nmol/l)	n.d.		370					
Luteinizing hormone (LH) (IU/L)	4.2*	<0.2	7.5*	<3.3			2.9	<3.3
Follicle-stimulating hormone (FSH) (IU/L)	7.7*	0.5–5.5	7.0*	<6			6.0*	<6
Prolactin (ug/L)			13	3–19				
Estradiol (pmol/L)	58	<160	126*	<73			73*	<73
Dehydroepiandrosterone sulfate (DHEAS) (umol/L)	1.3	<2.9	0.9	<2.9				
17-OHP (nmol/L)	0.8	<1.0	1.7*	<1.0				
Androstenedione (nmol/L)	2.6*	<0.917	4.2*	<0.917				
Testosterone (nmol/L)	<0.3	<3.9						
IGF-1 (ug/L)			599*	87–324	727*	87–324		

DEXA scan results at time point 5 (bone age approximately 3 years older) and time point 9 (bone age 2-2.5 years older)				
Region	**Time point 5 % Fat**	**Time point 5 % Fat centile**	**Time point 9 % Fat**	**Time point 9 % Fat centile**
Left arm	49.3	92nd	51.6	95th
Right arm	50.1	93rd	47.3	89th
Trunk	36.3	86th	38.0	88th
Left leg	47.0	91st	44.1	81st
Right leg	49.8	95th	47.9	92nd
Subtotal	42.3	89th	42.3	89th
Head	27.5		27.3	
Total	40.7	89th	40.9	89th
Android	44.8		42.3	
Gynoid	47.1		46.0	

*Outside of reference range.
n.d, not done; 17-OHP, 17-hydroxyprogesterone.

(BC) Children's Hospital for precocious puberty and short stature (table 1). This study involved a human participant and written informed consent was obtained from the legal guardians through an Institutional Review Board (IRB)-approved research protocol 'Comprehensive Characterisation of Genetic Disorders of Body Weight' (Certificate H08-00784). Karyotyping excluded chromosomal rearrangement.

Prior clinical chromosomal microarray analysis had found a 77 megabase run of homozygosity (RoH) on Chr14, thought to represent UPD 14; based on the phenotype, segmental maternal UPD14 was deemed likely. Clinical laboratory analysis was done of microsatellite markers D14S67 and D14S250 from the patient and both parents, at GRCh38 regions chr14:87921456–87921846 and chr14:99991912–99992256, respectively, within the RoH. These two markers were consistent with maternal isodisomy. Microsatellite markers D14S72, D14S50 and D14S283 (at chr14:20902829–20903192, chr14:21887644–21887913 and chr14:22219508–22219885, respectively) were also analysed, though these lay outside the RoH found on microarray. Informative markers outside the RoH were consistent with biparental inheritance. Subsequent cytogenetic analysis of cultured peripheral blood lymphocytes showed a normal female karyotype.

Research-grade dual-energy X-ray absorptiometry (DEXA) scans reported here used Hologic Horizon A with Apex Software V.5.6.1.3. Internal reference data were calibrated against National Health and Nutrition Examination Survey data.[13]

Nanopore sequencing

DNA was extracted from patient blood using the MagAttract high-molecular-weight (HMW) DNA kit (Qiagen). High Pass Plus Cassette and the SAGE Science Blue Pippin instrument selected DNA lengths of 15 000–150 000 base pairs. DNA libraries were then built using Genomic DNA by Ligation (SQK-LSK110) protocol. ~1 µg of HMW DNA was used for ONT PromethION genome sequencing using kit 14 chemistry for 72 hours with R10.4.1 flow cells. Flow cells were flushed between 24 hours and 48 hours using DNase I nuclease (Invitrogen) before being reloaded with the patient library.

Bioinformatics

Nanopore data analysis was performed using two NVidia A6000 graphics processing units. Dorado-0.3.4 with dna_r10.4.1_e8.2_400bps_sup@v4.2.0 model was used for simultaneous base calling, methylation calling, and alignment (GRCh38 reference genome) of nanopore PromethION sequencing data using the parameters --device cuda:0 -- modified-bases 5mCG_5hmCG.[14] Single-nucleotide variants (SNVs) and small insertions and deletions were called using Clair3 V.0.1-r8.[15] Haplotype tagging of reads was done using WhatsHap Haplotag V.1.2.[16] For B allele frequency (BAF) plots, SNVs with a minimum of 10 read supports were used. Moreover, to enable SNV visualisation, we only plotted regions that were present in the Illumina Infinium OmniExpress-24 V.1.3 variant region file.[17] Delly V.0.8.7 bioinformatics tool was used to assess DNA copy number (CN) using the mappability file Homo_sapiens.GRCh38.dna.primary_assembly.fa.r101.s501.blacklist.gz.[18] Methylation was included in Dorado-0.3.4 basecalling and stored in the aligned bam file; methylation analysis was done visually using phased bam files, with the methylation tag in Integrative Genomics Viewer (IGV) V.2.16.1.[19] The Temple syndrome ICRs and other Chr14 imprinting regions were determined from published literature.[20] Details of PromethION sequencing are found in online supplemental table 1. The absence of structural variants in the relevant regions was determined through the bioinformatics tool Sniffles V.2.0.7 and visually through IGV.[21]

RESULTS

Clinical phenotype

The proposita was born of non-consanguineous parents via emergency caesarean section for failed labour induction. Pregnancy had been complicated by postdates and intrauterine growth restriction. Her birth weight was in the first percentile (−2.4 SD). She had no complications or congenital anomalies except for transient breathing difficulties. She did not need resuscitation or assisted feeding. There was no gestational diabetes mellitus, history of hypoglycaemia, poor tone or poor feeding in the early neonatal period. Postnatally, she exhibited persistent growth failure, remaining at the 0.3rd percentile for weight and height. Assessment showed left metatarsus adductus in infancy that resolved with parent-facilitated stretching. She had normal to advanced skill acquisition in all domains, with no speech delays or behavioural difficulties.

Signs of puberty reportedly began around age 6–10 years (time point 1), with the appearance of breast buds and possible pubic hair. A year later, she was assessed to be prepubertal with Tanner 1 breast formation (time point 2); 3 months following that, she had Tanner 2 breast development, body odour and acne (time point 3). A couple of months following Tanner 2 breast development, she experienced menarche.

A month after menarche (time point 4), her height was at the 71st percentile (Z-score +0.53 SD), and her weight was at the 83rd percentile (+0.9 SD). Head circumference was at the 72nd percentile (+0.57 SD), and upper segment to lower segment ratio was 0.975. Blood pressure was 114/64 mm Hg (mean arterial pressure 81 mm Hg) and heart rate 86 bpm. Physical exam found normocephaly, a rounded face, a normal nasal bridge, a high arched palate, crowded teeth, normal phalanges and normal palmar creases. She had some upper forehead acne, but no hirsutism. She was Tanner 4 for pubic hair development and Tanner 3 for breast development. Brain MRI showed no pituitary or other central lesion, and ultrasound of the adrenal glands, uterus and ovaries found a small ovarian cyst that disappeared within 4 months.

At time point 2, prior bone age (BA) was initially read as normal; subsequent review placed it between the Greulich and Pyle standards of 2–3 years older. By time point 4, follow-up BA was closest to the Greulich and Pyle standards of 2.5–3 years older. Insulin-like growth factor 1 (IGF-1) was elevated at 599 ug/L.

Three months after time point 4 (time point 5), growth parameters indicated the 68th percentile (+0.48 SD) for height for CA, but the second percentile (−2.0 SD) for BA of approaching 3 years older. Her weight was at the 81st percentile (+0.89 SD) for CA, but 17th percentile (−0.94 SD) for BA. Her body mass index was at the 82nd percentile (+0.91 SD) for CA, but 56th percentile (+0.15 SD) for BA. Though these growth parameters were within the age-appropriate range for a European-derived population, there was concern her final height would be below the third percentile, given her significantly advanced BA and the rapidity of her pubertal progression. Though a formal estimation could not be made because of her underlying epigenetic condition, her mid-parental height (assumed polygenic background) was at the 96.5th percentile, based on paternal and maternal heights (menarche at age 12–13 years). FSH and LH levels showed evidence of central puberty (table 1).

A month after time point 5 (time point 6), height had increased to the 73rd percentile and +0.6 SD for CA, and weight had increased to the 85th percentile and +1.0 SD for CA. BMI was at the 85th percentile and +1.0 SD for CA. Comparing with the measurement from previous timepoints, her annualised linear growth velocity had been 7.2 cm per year. Once the UPD14 diagnosis was suggested from microarray results, the parents agreed to temporary pubertal blockade and growth hormone therapy to try to maximise height potential by preventing further BA advancement while promoting growth. Informed consent for these clinical therapies was obtained. A month following time point 6, after a case conference, she was given leuprolide acetate for depot suspension 7.5 mg intramuscular, with planned dosing at every 4 weeks. A month after starting leuprolide acetate for depot suspension, she was given 0.2 mg/kg/week of human growth hormone (time point 7). Prior to medication start, a DEXA scan was done (table 1, online supplemental table 2).

One month after starting growth hormone (time point 8), leuprolide acetate for depot suspension and growth hormone were stopped due to a supraphysiological IGF-1 of 727 ug/L and new-onset headaches and abdominal pain. Although there was no evidence of papilloedema on ophthalmological exam, there was concern about the possibility of raised intracranial pressure.

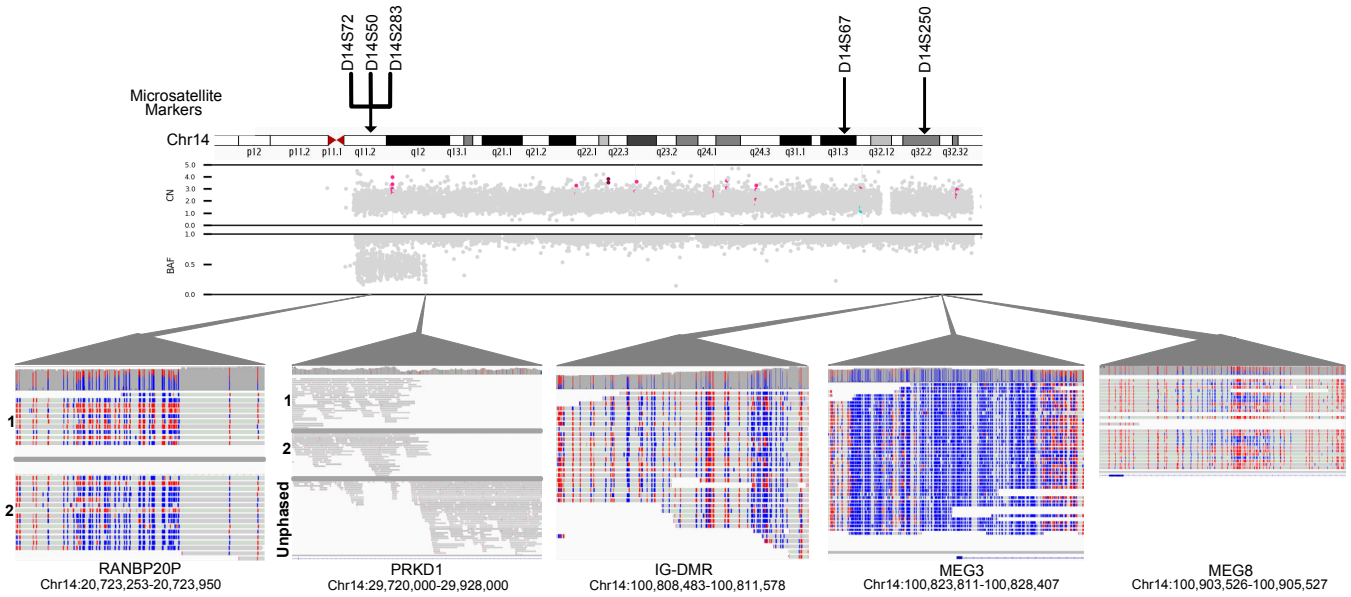

Figure 1 Patient with Temple syndrome with mixed maternal UPD. On the uppermost part, an ideogram shows regions of chromosome 14. Below this, the CN plot demonstrates a normal CN across Chr14, while the BAF plot shows a proximal centromeric heterozygosity and homozygosity from 14q12 to the telomere of Chr14. On the bottom from left to right, IGV screenshots of nanopore reads showing the methylation status at known maternally methylated *RANBP20P*, approximate breakpoint region within *PRKD1*, paternally methylated IG-DMR and *MEG3*, and maternally methylated *MEG8* imprinted regions. Identifying exact breakpoints was not possible as the reads spanning the breakpoints were in a difficult-to-map region. However, the presence of two haplotypes followed by the loss of allelic phasing as a result of the loss of heterozygous variants is present in the figure. In the nanopore reads, red indicates methylated CpGs and blue indicates unmethylated CpGs. BAF, B allele frequency; Chr14, chromosome 14; CN, copy number; IGV, Integrative Genomics Viewer; UPD, uniparental disomy. The gap with no data points in the CN plot is the region ignored by the CN caller, Delly, based on the required GRCh38 mappability map file.

The family elected to stop all treatment, after which her headaches and abdominal pain resolved within a few days.

At follow-up assessment (time point 9), which was 3 months after time point 8, height had increased to the 78th percentile and +0.77 SD for CA, and weight had increased to the 89th percentile and +1.24 SD for CA. BMI was at the 89th percentile and +1.23 SD for CA. Head circumference was at the 25th percentile and −0.68 SD for CA. BA was assessed as 2–2.5 years older, having advanced by 1 SD over the preceding several months. Follow-up DEXA scan was also done (table 1 and online supplemental table 2).

Long-read sequencing subtyping

To determine genetic abnormalities, we explored changes in CN and used BAF to explore variant zygosity. The CN plot demonstrated normal CN (CN∼2) across Chr14. The BAF plot demonstrated a RoH (BAF∼1) across Chr14 (near the middle of 14q12 to the end of the long arm) except for a proximal centromeric heterozygous region (figure 1). We examined DNA methylation at three ICRs at the RoH region, including paternally methylated *MEG3*/*DLK1* (IG-DMR) and *MEG3*:TSS and maternally methylated *MEG8*.[20] CpG sites demonstrated substantially diminished methylation at IG-DMR and a lack of methylation at *MEG3*:TSS, while showing substantial methylation at *MEG8* (figure 1). These data suggest maternal isodisomy for the RoH region. To examine the parent of origin of the proximal centromeric heterozygous region without parental data, we used the maternally methylated *RANBP20P* imprinted region.[20 22] At this region, we observed differential allelic methylation suggesting the presence of both parental alleles (figure 1). This is consistent with the clinical report and biparental inheritance of the heterozygous region arising through postzygotic mitotic recombination. Altogether, these results suggest maternal isodisomy for the majority of Chr14 with a proximal centromeric biparental region.

DISCUSSION AND CONCLUSION

Temple syndrome is a rare imprinting disorder caused by aberrant expression of imprinted genes at chromosome 14q32. Timely and accurate molecular diagnosis aids with management of phenotypical implications such as precocious puberty; subtyping of Temple syndrome assists recurrence risk estimation. Using solely whole genome long-read sequencing of the proposita for diagnostic interpretation, we resolved the molecular cause of a Temple syndrome case where clinical diagnostic testing had required parental samples. Methylation analysis of the imprinted regions at 14q32 including paternally methylated *MEG3*/*DLK1* (IG-DMR) and *MEG3*:TSS and maternally methylated *MEG8* supported the maternal origin of both copies of the isodisomy region. However, DNA methylation of some CpG sites at *MEG3*/*DLK1* (IG-DMR) and some reads at *MEG8* imprinted regions were not consistent with maternal origin of the isodisomy segment. *MEG3*/*DLK1* is reported to function in placenta,[23] which might explain the discordance between expected methylation and the methylation observed at some CpG sites in blood-derived DNA. It is possible that imprinted methylation is more conserved in placenta than in other embryonic tissues, where stochastic methylation errors affect imprinted methylation of some CpG sites. *MEG8* is reported to be a somatic imprinted region,[20 24] which might explain the presence of a few reads with inconsistent methylation across the imprinted region. These inconsistently methylated reads suggest the establishment

of *MEG8* imprinted methylation at latter postfertilisation cycles and the presence of a mosaic pattern where some of the cell populations lack imprinted methylation. By examining the methylation at the *RANBP20P* imprinted region, we concluded that the heterozygous region of Chr14 shows biparental inheritance because it demonstrated the expected biparental methylation, a maternally methylated allele and a paternally unmethylated allele. The ICRs at *MEG3/DLK1*, *MEG3:TSS* and *MEG8* have been reported by several studies, giving evidence to their stability. In contrast, *RANBP20P* allele-specific methylation is not reported in several studies and demonstrated variation across individuals, suggesting this is a polymorphic imprinted region and some individuals may not have *RANBP20P* imprinted methylation.[20] Therefore, even though the presence of allelic methylation at this ICR suggests biparental inheritance, the absence of allelic methylation does not rule out biparental inheritance; further validation by STR analysis would be needed to ascertain that the *RANBP20P* region was biparentally contributed. Although our data were sequenced on the PromethION instrument, Oxford Nanopore's ability to detect DNA methylation and imprinting is shown using other instruments, such as the MinION. Therefore, we expect this work to be applicable across different Nanopore instruments.[10 25] However, the ONT minION produces substantially less yield than the promethION, therefore several more flow cells would be needed to obtain the comparable amount of data necessary for determining phasing and imprinting.[26] Nanopore also has limitations, such as identifying indels in regions with homopolymers and requiring high nucleic acid inputs.[26 27]

We have also examined DNA methylation in this sample at other established imprinted regions across the genome to investigate a global or multilocus imprinting disturbance.[22] DNA methylation at the imprinted regions in this sample demonstrated allele-specific DNA methylation with similar distribution to 12 normal lymphoblastoid cell line samples,[20] ruling out the possibility of a genome-wide imprinting disturbance (online supplemental figure 1).

This patient's phenotype appears milder than that of many reported cases, since she lacked feeding difficulties, developmental delays, hypotonia or behavioural difficulties such as hyperphagia. Some component of the phenotypical subtlety likely derives from the presence of segmental matUPD, rather than UPD along the entire length of Chr14. The identification of separate 'critical regions' for these endophenotypes must await larger data sets that match epigenotypes to detailed phenotypical information.

In summary, we demonstrated the application of nanopore sequencing as a one-step approach to diagnose and subtype a case with Temple syndrome. To our knowledge, this is the first report of a Temple syndrome resolved solely by long-read nanopore sequencing in a proposita without any parental data, thereby providing proof of concept and workflow for the molecular diagnosis of this syndrome using long-read sequencing.

Author affiliations
[1]Canada's Michael Smith Genome Sciences Centre, BC Cancer, Vancouver, British Columbia, Canada
[2]Bioinformatics Graduate Program, University of British Columbia, Vancouver, British Columbia, Canada
[3]Department of Medical Genetics, Faculty of Medicine, University of British Columbia, Vancouver, British Columbia, Canada
[4]BC Children's Hospital, Vancouver, British Columbia, Canada
[5]Division of Endocrinology, Department of Pediatrics, University of British Columbia, Vancouver, British Columbia, Canada
[6]Program in Genetics and Genome Biology, The Hospital for Sick Children, Toronto, Ontario, Canada
[7]Department of Molecular Genetics, University of Toronto, Toronto, Ontario, Canada
[8]Provincial Medical Genetics Program, BC Women's Hospital, Vancouver, British Columbia, Canada
[9]Department of Pathology and Laboratory Medicine, University of British Columbia, Vancouver, British Columbia, Canada
[10]BC Children's Hospital Research Institute, Vancouver, British Columbia, Canada
[11]School of Kinesiology, University of British Columbia, Vancouver, British Columbia, Canada

Acknowledgements The authors thank the many groups at Canada's Michael Smith Genome Sciences Center, including Laboratory Information Management System (LIMS), Biospecimen, Sequencing, Bioinformatics, Purchasing, and Project Management teams for their contribution.

Contributors SD and VA were responsible for data analysis and manuscript writing. SJMJ, WTG, KD, YS, CFB, SC, RW, DF, VA, SD were responsible for funding acquisition. WTG, DH, DF, DG, LS recruited and consented patients and contributed to phenotype analysis. KSB and ES contributed to clinical laboratory analysis. SJMJ and WTG contributed resources and were responsible for supervision. All authors reviewed and edited the manuscript. This project was jointly conceived among all authors.

Funding This work was partially funded by the Canadian Institutes of Health Research grants PJT-168982 and PJT-185999. SD and VA are funded through the BC Cancer Agency Rising Stars initiative. SJMJ has been given funding through the Canada Research Chairs programme. WTG gratefully acknowledges funding from the BC Children's Hospital Research Institute IGAP award.

Competing interests Travel funding for conference presentations has been given to SD, KD and SJMJ from Oxford Nanopore. YS, SC, RW, CFB and SJMJ are affiliated with Alamya Health, which provides genetic sequencing using Oxford Nanopore technology. All the other authors have no relevant disclosures.

Patient consent for publication Not applicable.

Ethics approval This study involves human a participant and was approved by the University of British Columbia Research Ethics Committee. The family provided informed consent under REB #H08-00784. Participants gave informed consent to participate in the study before taking part.

Provenance and peer review Not commissioned; externally peer reviewed.

DNA methylation frequency data are available at the Federated Research Data Repository under DOI: 10.20383/103.0963. Other data are not publicly available to retain patient confidentiality; however, data can be obtained from the corresponding author upon reasonable request.

ORCID iDs
Sarah Dada http://orcid.org/0000-0002-3445-2377
Vahid Akbari http://orcid.org/0000-0001-8005-7776
William T Gibson http://orcid.org/0000-0002-6552-402X

REFERENCES

1 Kagami M, Nagasaki K, Kosaki R, *et al*. Temple syndrome: comprehensive molecular and clinical findings in 32 Japanese patients. *Genet Med* 2017;19:1356–66.
2 Yordanova N, Iotova V, Mackay DJG, *et al*. Long-term Follow-up of a Late Diagnosed Patient with Temple Syndrome. *J Clin Res Pediatr Endocrinol* 2024;16:475–80.
3 Yordanova N, Iotova V, Mackay DJG, *et al*. Long-term Follow-up of a Late Diagnosed Patient with Temple Syndrome. *J Clin Res Pediatr Endocrinol* 2022;0.
4 Ioannides Y, Lokulo-Sodipe K, Mackay DJG, *et al*. Temple syndrome: improving the recognition of an underdiagnosed chromosome 14 imprinting disorder: an analysis of 51 published cases. *J Med Genet* 2014;51:495–501.
5 Juriaans AF, Trueba-Timmermans DJ, Kerkhof GF, *et al*. The Effects of 5 Years of Growth Hormone Treatment on Growth and Body Composition in Patients with Temple Syndrome. *Horm Res Paediatr* 2023;96:483–94.

6 Juriaans AF, Kerkhof GF, Mahabier EF, *et al*. Temple Syndrome: Clinical Findings, Body Composition and Cognition in 15 Patients. *J Clin Med* 2022;11:6289.
7 Eggermann T, Monk D, de Nanclares GP, *et al*. Imprinting disorders. *Nat Rev Dis Primers* 2023;9:33.
8 Prasasya R, Grotheer KV, Siracusa LD, *et al*. Temple syndrome and Kagami-Ogata syndrome: clinical presentations, genotypes, models and mechanisms. *Hum Mol Genet* 2020;29:R107–16.
9 Kagami M, Yanagisawa A, Ota M, *et al*. Temple syndrome in a patient with variably methylated CpGs at the primary MEG3/DLK1:IG-DMR and severely hypomethylated CpGs at the secondary MEG3:TSS-DMR. *Clin Epigenetics* 2019;11:42.
10 Akbari V, Garant J-M, O'Neill K, *et al*. Megabase-scale methylation phasing using nanopore long reads and NanoMethPhase. *Genome Biol* 2021;22:68.
11 Akbari V, Dada S, Shen Y, *et al*. Long-read sequencing for detection and subtyping of Prader-Willi and Angelman syndromes. *J Med Genet* 2024;62:32–6.
12 Yamada M, Okuno H, Okamoto N, *et al*. Diagnosis of Prader-Willi syndrome and Angelman syndrome by targeted nanopore long-read sequencing. *Eur J Med Genet* 2023;66:104690.
13 Hinton BJ, Fan B, Ng BK, *et al*. Dual energy X-ray absorptiometry body composition reference values of limbs and trunk from NHANES 1999-2004 with additional visualization methods. *PLoS One* 2017;12:e0174180.
14 Li H. Minimap2: pairwise alignment for nucleotide sequences. *Bioinformatics* 2018;34:3094–100.
15 Zheng Z, Li S, Su J, *et al*. Symphonizing pileup and full-alignment for deep learning-based long-read variant calling. *Nat Comput Sci* 2022;2:797–803.
16 Martin M, Patterson M, Garg S, *et al*. WhatsHap: fast and accurate read-based phasing. *Bioinformatics* [Preprint] 2016.
17 Illumina. Infinium omniexpress-24 v1.3 support files. Available: https://support.illumina.com/downloads/infinium-omniexpress-24-v1-3-support-files.html [Accessed 10 Jul 2024].
18 Rausch T, Zichner T, Schlattl A, *et al*. DELLY: structural variant discovery by integrated paired-end and split-read analysis. *Bioinformatics* 2012;28:i333–9.
19 Robinson JT, Thorvaldsdóttir H, Winckler W, *et al*. Integrative genomics viewer. *Nat Biotechnol* 2011;29:24–6.
20 Akbari V, Garant J-M, O'Neill K, *et al*. Genome-wide detection of imprinted differentially methylated regions using nanopore sequencing. *Elife* 2022;11:e77898.
21 Smolka M, Paulin LF, Grochowski CM, *et al*. Detection of mosaic and population-level structural variants with Sniffles2. *Nat Biotechnol* 2024;42:1571–80.
22 Akbari V, Hanlon VCT, O'Neill K, *et al*. Parent-of-origin detection and chromosome-scale haplotyping using long-read DNA methylation sequencing and Strand-seq. *Cell Genom* 2023;3:100233.
23 Kagami M, O'Sullivan MJ, Green AJ, *et al*. The IG-DMR and the MEG3-DMR at human chromosome 14q32.2: hierarchical interaction and distinct functional properties as imprinting control centers. *PLoS Genet* 2010;6:e1000992.
24 Monk D, Morales J, den Dunnen JT, *et al*. Recommendations for a nomenclature system for reporting methylation aberrations in imprinted domains. *Epigenetics* 2018;13:117–21.
25 Liu Y, Rosikiewicz W, Pan Z, *et al*. DNA methylation-calling tools for Oxford Nanopore sequencing: a survey and human epigenome-wide evaluation. *Genome Biol* 2021;22:295.
26 Wang Y, Zhao Y, Bollas A, *et al*. Nanopore sequencing technology, bioinformatics and applications. *Nat Biotechnol* 2021;39:1348–65.
27 Kolmogorov M, Billingsley KJ, Mastoras M, *et al*. Scalable Nanopore sequencing of human genomes provides a comprehensive view of haplotype-resolved variation and methylation. *Nat Methods* 2023;20:1483–92.